THE JOURNAL OF PHYSICAL CHEMISTRY C

Article

pubs.acs.org/JPCC

Spectroscopy and Dynamics of the Multiple Free OH Species at an Aqueous/Hydrophobic Interface

Ali Eftekhari-Bafrooei,[†] Satoshi Nihonyanagi,[‡] and Eric Borguet*

Department of Chemistry, Temple University, Philadelphia, Pennsylvania 19122, United States

Supporting Information

ABSTRACT: Sum frequency generation (SFG) spectra and free induction decay (FID) measurements of the H_2O/octadecylsilane (ODS)/silica interface in the free OH spectral region (~3700 cm^{-1}) show spatially inhomogeneous behavior. The SFG spectra and FIDs suggest an inhomogeneous response of the free OH, consisting of at least two distinct species at the interface with short and long coherence times. In most areas of the sample, an OH band at ~3680 cm^{-1} with a short dephasing (<150 fs), assigned to the free OH of water interacting with the hydrophobic methyl group of ODS, was observed in agreement with previously reported SFG spectra of the H_2O/ODS/silica interface. In a small fraction (~20%) of the sample areas, a more intense peak at ~3700 cm^{-1} was observed in the SFG spectrum characterized by significantly longer dephasing (~760 fs) in the SFG-FID. Based on the peak position, as well as control experiments on octadecydimethylmethoxysilane (ODMS) monolayers and deuterium substitution experiments at the water/ODS/silica interfaces, two possible assignments for the new feature are provided. The long dephasing can be due to the free OH of the Si−OH of incompletely cross-linked/tethered ODS molecules. Alternatively, a contribution of water molecules trapped in nano pores of silica surface and/or confined between the ODS molecules can explain the long coherence. Either way, the long coherence can be attributed to the OH species decoupled from bulk water.

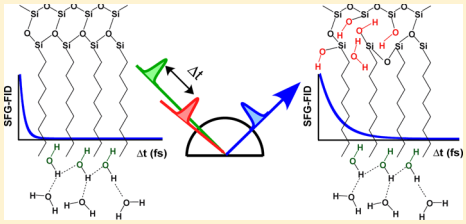

INTRODUCTION

Interfacial water plays an important role in a variety of disciplines including physics, chemistry, biology, geology, and atmospheric sciences.[1−3] At solid/liquid interfaces, the structure and dynamics of water is influenced by the properties of the solid surface such as hydrophobicity. Molecular level elucidation of the interaction between water and hydrophobic surfaces is particularly important to understand biological phenomena such as protein folding, which is known to be mediated by the first layer of water next to apolar groups.[4] One of the fundamental questions regarding the interaction of water with hydrophobic surfaces is whether or not there is a depleted layer of water near the hydrophobic surface.[5−7] MD simulations predict a local density fluctuation of water near the surface.[8,9] These studies suggest cavity formation near hydrophobic surfaces and that the cavity formation is suppressed near hydrophilic surfaces.[8,9] From an experimental point of view, both neutron reflection[10,11] and X-ray reflection measurements[12−14] suggest the existence of a layer with reduced water density near hydrophobic surfaces. The thickness of the depleted layer depends on the dissolved gas and the nanoscale properties of the surface.[10,14] Nevertheless, the details of the depleted water density and cavity formation near hydrophobic surfaces are still elusive and remain under debate. Resolving this issue as well as controlling and manipulating hydrophobic/hydrophilic interactions, which are important in many technical and biomedical applications, requires a molecular level understanding of the structure and dynamics of water at these surfaces.[15]

Silicon dioxide (silica) is one of the most abundant natural minerals on the planet. The silica surface is characterized, in significant part, by interfacial silanol groups (SiOH) that are believed to be the origin of silica's hydrophilic properties. Modification of silica surfaces with hydrophobic siloxane self-assembled monolayers (SAMs) has been a topic of interest in many research groups since the first report of an ordered monolayer formation on silica.[16,17] Octadecylsilane (ODS), a prototypical SAM, has been extensively used to study water structure at hydrophobic surfaces.[12,13,18−20]

Since the interfacial water molecules comprise only a few molecular layers, probing the structure, orientation, and changes in composition of the interfacial region calls for sensitive interface-specific methods. Optical techniques based on second-order nonlinear processes, namely second-harmonic generation (SHG) and sum-frequency generation (SFG), have become ideal probes of liquid interfaces.[21−24] The interface specificity of SHG and SFG lies in the fact that second-order optical processes are forbidden in centrosymmetric media in the dipole approximation but are allowed when the inversion symmetry is broken, e.g., at liquid interfaces.

Vibrational SFG (VSFG) spectra of water at various interfaces have been acquired by several research groups.[21] In the hydrogen-bonded OH stretch region, two distinct vibrational features at ~3200 and 3400 cm^{-1} have been observed in

Received: October 20, 2011
Revised: May 7, 2012
Published: May 30, 2012

the VSFG of almost all water interfaces.[18,25−34] In the non-hydrogen-bonded region of water, a distinct sharp feature near 3700 cm^{-1} is observed for water/hydrophobic interfaces, e.g., air/water,[29,32,35−38] air/ice,[39] oil/water,[40,41] and water in contact with SAMs,[18,25,42] and has been assigned to the free or dangling OH bond, i.e., an OH bond that is not hydrogen bonded to other water molecules and straddles the interface between the bulk water and the hydrophobic phase.

The free OH band at the water/ODS/silica interface has been reported in SFG spectra by several groups.[18,20,25,42] In all cases, a single free OH peak was observed near 3680 cm^{-1}.[23] In the absence of water, i.e., ODS in dry air, strong peaks attributed to free silanols were observed at ∼3708 and 3792 cm^{-1} in the SFG spectra of the air/ODS/silica interface.[43] Because the frequencies of the distinct species are close to each other, it is worth considering the possibility that the SFG spectra (especially in the case of broad-band SFG where the resolution of the spectra is determined by the bandwidth of the visible pulse) cannot resolve two peaks and only one frequency is observed in the SFG spectrum of the water/ODS/silica interface. Time domain SFG is complementary to, and in some cases more informative than, frequency domain SFG.[44−47] Combining frequency domain SFG (SFG spectra) and time domain SFG (SFG-free induction decay, FID) may then provide insight into the properties, structure and the dephasing dynamics, of each of these species at the water/OTS/silica interface in the free OH region.

In this study, we report the SFG spectra (frequency domain) and SFG-FID (time domain) of water in contact with ODS SAMs on silica in the free OH region (∼3700 cm^{-1}). Both the SFG spectra and the SFG-FID in the free OH region show spatially heterogeneous behavior across the interface. In particular, a long coherence in the SFG-FID of free OH region was observed in certain spatial regions of the sample. We believe that this is due to a species that is distinct from the free OH of water in contact with the hydrocarbon chains of ODS, which has a short dephasing time. Although a unique assignment for the species giving rise to the long coherence is challenging, free OH species including the Si−OH groups of ODS (alkyl-SiOH) or silica (silica-SiOH), and water trapped underneath the ODS monolayer are plausible candidates for the long dephasing free OH vibration at the H_2O/ODS/silica interface.

EXPERIMENTAL SECTION

An IR-grade fused silica prism (IRFS, ISP optics) was cleaned by piranha solution (3:1 (v/v), concentrated sulfuric acid and 30% hydrogen peroxide (*Caution! Piranha solution is a very strong oxidant and can be dangerous to work with; gloves, goggles, and a face shield should be worn*)), rinsed with copious amounts of DI water, and dried by a stream of pure nitrogen prior to SAM formation. The ODS SAM was prepared by immersing the clean IR fused silica prism for 20 min into 2.5 mM octadecyltrichlorosilane (OTS, Gelest Inc.) solution in (3:1) hexadecane (Sigma, >99%) and $CHCl_3$ (Sigma Aldrich, 99.8%).[48−50] The ODS-coated prism was rinsed with $CHCl_3$ and dried with a stream of pure nitrogen. The octadecyldimethylmethoxysilane (ODMS) SAM was prepared by immersing the clean IR fused silica prism into 10 mM of ODMS (Gelest Inc.) solution in hexane (Sigma, >99%) for 6 h. The ODMS-coated prism was then rinsed with hexane at least three times and dried with a stream of pure nitrogen. The pH of water was ∼6 for all of the measurements.

Details of the experimental setup for SFG measurements can be found elsewhere.[51] Briefly, a commercial optical parametric amplifier (TOPAS, Light Conversion) provides femtosecond IR pulses for frequency and time domain SFG measurements. The TOPAS was pumped by 90% of the output of a femtosecond regenerative amplifier (Quantronix, Integra-E; central wavelength 814 nm, repetition rate 1 kHz, pulse width ∼130 fs fwhm, pulse energy ∼3 mJ). The remaining 10% of the amplifier output was used as a visible pulse for the SFG measurements. For the time domain SFG, the energy and the polarization of the visible pulse were adjusted by a combination of a half-wave plate and a prism polarizer. For the frequency domain measurements, the bandwidth of the visible pulse was reduced to ∼14 cm^{-1} by passing through two narrow band-pass filters (CVI). The IR and visible beams, with energies of ∼8 and 2 μJ/pulse, incident at the surface with angles of 72° and 65°, were focused to beam waists of 250 and 200 μm, respectively. The polarization of IR beam was p-polarized whereas the visible and SFG beams were either s- or p-polarized as described in the text. The SFG signal was separated from the reflected visible light by short-pass filters (Melles Griot) and was detected by a CCD detector (Princeton Instruments) coupled with a spectrograph (300i, Acton Research Corp.). The SFG spectral response was recorded from a gold-coated IR fused silica prism for normalization purposes. The frequency axes of the spectra were calibrated by correlating the IR absorption in the C−H stretching region of a standard polystyrene film and the corresponding dips in the SFG spectra when the film was placed in the IR path for SFG measurements. For the SFG-FID measurements, the SFG intensity was integrated over a region of interest in the CCD using a custom-written LABVIEW 8 program. Data analysis was performed using Matlab 7 (MathWorks). In order to avoid IR absorption in the free OH region, and also eliminate the possibility that some peaks in the SFG spectra in the free OH region are artifacts due to IR absorption by water vapor, all experiments were done at low humidity (∼5%) achieved by purging the beam path.

FITTING PROCEDURE

(a). Normalized SFG Spectra. For the SFG spectra only (SFG spectra in the C−H stretching region), the normalized spectra were fit to the following equation[35,52]

$$I_{SFG} \propto \left| \sum_n \frac{A_n}{\omega_{IR} - \omega_n + i\left(\Gamma_n + \frac{\Delta\omega_{vis}}{2}\right)} + |A_{NR}|e^{i\varepsilon} \right|^2 \quad (1)$$

where ω_{IR} is the center frequency of the IR pulse and A_n, ω_n, and Γ_n are the amplitude, frequency, and damping constant of the nth surface vibrational mode, respectively. A_{NR} and ε are the amplitude of the nonresonant component and the phase between the resonant and nonresonant contributions. $\Delta\omega_{vis}$ is the bandwidth of the visible pulse and is added to Γ_n to account for the spectral resolution of the broad-band SFG measurement, set by the finite visible bandwidth.

(b). Simultaneous Fit of SFG Spectra and FID without Inhomogeneous Contribution. For the simultaneous fit, unnormalized spectra and FID were used. A slightly modified version of eq 1 was used for the fit of SFG spectrum

$$I_{SFG} \propto \left| \sum_n \frac{A_n}{\omega_{IR} - \omega_n + i\left(\Gamma_n + \frac{\Delta\omega_{vis}}{2}\right)} + \frac{|A_{NR}|}{\Delta\omega_{IR}} e^{i\varepsilon} \right|^2 \exp\left\{ -\left(\frac{\omega_{IR} - \omega_0}{\Delta\omega_{IR}} \right)^2 \right\} \quad (2)$$

where the exponential term describes the Gaussian-shaped spectrum of the incident IR pulse. ω_0 and $\Delta\omega_{IR}$, which represent the center frequency and spectral width of the IR pulse, respectively, were estimated independently from the SFG spectrum of a gold-coated silica prism under the same experimental geometry.

The intensity of time domain SFG (SFG-FID) as a function of delay time (t_d) between IR and visible pulses can be written as

$$I_{SFG-FID}(t_d) \propto \int_{-\infty}^{\infty} dt\ |P^{(2)}(t, t_d)|^2 \quad (3.1)$$

$$P^{(2)}(t, t_d) \propto E_{vis}(t - t_d) P^{(1)}(t) \quad (3.2)$$

$$P^{(1)}(t) = \int_{-\infty}^{\infty} dt'\ E_{IR}(t - t') S(t') \quad (3.3)$$

where $P^{(1)}$, $P^{(2)}$, and $S(t)$ are the first-order polarization, the second-order polarization, and the response function of the system, respectively. E_{vis} and E_{IR} are the electric fields of the visible and IR pulses characterized by Gaussian spectral and temporal profiles. The response function of the system can be written as

$$S(t) = [\delta(t)|A_{NR}| \exp(i\varepsilon) - i\theta(t) \sum_n A_{R,n} \exp(2\pi c(-i\omega_n t - \Gamma_n t))] + cc \quad (3.4)$$

where $\delta(t)$ is the delta function, $\theta(t)$ is the Heaviside step function, c is the speed of light and the inverse of $2\pi c\Gamma_n$ is the total dephasing time of nth vibrational mode ($T_{2,n}$).

(c). Simultaneous Fit of SFG Spectra and FID with Inhomogeneous Contribution. The nonexponential decay of the SFG-FID is usually an indication of the broadening of the homogeneous line width by an inhomogeneous contribution.[44] In this case an inhomogeneous line width (Γ_{inh}) is added to the homogeneous line width. In order to account for the inhomogeneous broadening in the SFG spectra fit function, a convolution of a Gaussian and a Lorentzian was assumed for each individual peak:

$$I_{SFG} \propto \left| \sum_n \mathrm{conv}\left(\frac{A_n}{\omega_{IR} - \omega_n + i\left(\Gamma_n + \frac{\Delta\omega_{vis}}{2}\right)}, \exp\left\{ -\left(\frac{\omega_{IR} - \omega_n}{\Gamma_{inh}} \right)^2 \right\} \right) + \frac{|A_{NR}|}{\Delta\omega_{IR}} e^{i\varepsilon} \right|^2 \exp\left\{ -\left(\frac{\omega_{IR} - \omega_0}{\Delta\omega_{IR}} \right)^2 \right\} \quad (4)$$

where conv is the convolution function and Γ_{inh} is associated with the inhomogeneous broadening of the nth vibrational mode centered at ω_n. Including the inhomogeneous broadening, the response function in the SFG-FID can then be written as

$$S(t) = [\delta(t)|A_{NR}| \exp(i\varepsilon) - i\theta(t) \sum_n A_{R,n} \exp(2\pi c(-i\omega_n t - \Gamma_n t)) * \exp(-(2\pi c\Gamma_{inh} t)^2)] + c.c \quad (5)$$

RESULTS AND DISCUSSION

The quality of the ODS SAMs was examined by measuring the water contact angle and the SFG spectra in the C−H stretching region. The contact angle of the ODS-coated prism was more than 105°, which is an indication of a hydrophobic surface. The SFG spectrum of an ODS-coated silica prism in contact with H_2O (pH ∼ 6) in the C−H stretching region for the ssp polarization combination (Figure 1a) is dominated by two major peaks at ∼2875 and ∼2936 cm^{-1}, assigned to the symmetric stretch and Fermi resonance of the terminal methyl

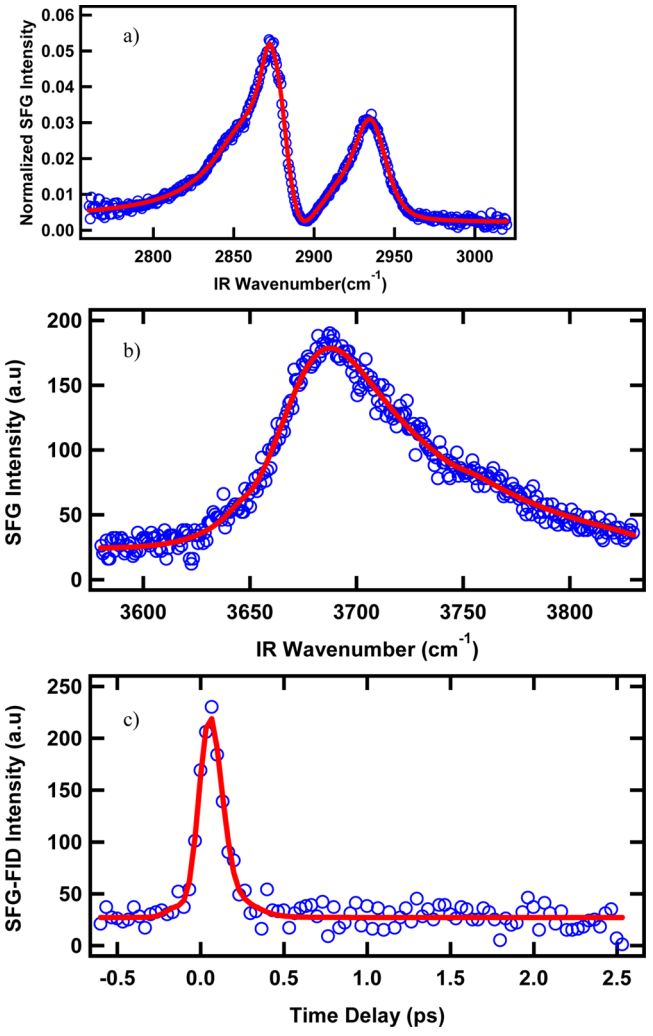

Figure 1. (a) SFG spectrum of ODS-coated silica interface in contact with H_2O in the C−H stretching region. (b) SFG spectrum and (c) SFG-FID of ODS-coated silica interface in contact with H_2O in the free O−H stretching region (∼3700 cm^{-1}). The polarization combination for SFG, vis, and IR is S,S,P.

dx.doi.org/10.1021/jp210090h | J. Phys. Chem. C 2012, 116, 21734−21741

group, in agreement with the previously reported SFG spectra of the same system.[18,53]

An accurate fit (using eq 1) of the spectrum requires the inclusion of additional modes (Table 1). The small amplitude

Table 1. Assignment, Amplitude, Line Width, and Frequency of Modes from the Fit of the SFG Spectrum of H_2O/ODS/Silica (Figure 1a) in the C−H Stretching Region

assignments	A_i	Γ_i (cm^{-1})	ω_i (cm^{-1})
CH_2-sym (d^+)	0.5	17	2855
CH_3-sym (r^+)	0.8	3	2875
t-CH_2 (t-$d^-(0)$)	−0.5	7	2889
CH_2-asym ($d^-(\pi)$)	0.02	3	2915
CH_3−FR (r^+_{FR})	1	8	2936
CH_3-asym (r^-)	−0.3	14	2950

of the bands at ∼2855 and ∼2915 cm^{-1}, assigned to the symmetric and asymmetric stretching of the methylene groups, suggests that there are few gauche defects in the SAM.[54] The band at ∼2950 cm^{-1} is assigned to the asymmetric stretching of the methyl group.[55] The band at 2888 cm^{-1} is assigned to the asymmetric stretching of the terminal methylene group next to silicon or the methyl group.[56] These spectroscopic features agree well with those previously reported, confirming the formation of a SAM of reasonably good quality.[18,53]

The non-normalized SFG spectrum and the SFG-FID of the ODS-coated silica prism in contact with H_2O (pH ∼ 6) in the free O−H stretching region (∼3700 cm^{-1}) are shown in Figure 1, b and c. A major peak at ∼3681 cm^{-1}, assigned to the free OH (dangling OH) of water molecules in contact with the methyl group of ODS, is observed in the SFG spectrum in agreement with previous SFG spectra.[18,20,25] The SFG-FID shows a fast response which is indistinguishable from the instrument function determined by the cross correlation of the IR and visible pulses on a gold-coated silica prism. The SFG spectrum and SFG-FID were fit simultaneously as described above and in detail elsewhere.[56]

The spectrum and FID could be fit with three frequencies at 3600, 3681, and 3780 cm^{-1} (Table 2). The dephasing of the

Table 2. Amplitude, Line Width, Dephasing, Frequency, and Inhomogeneous Broadening Line Width of the Modes from the Simultaneous Fit of the SFG Spectrum and the SFG-FID of H_2O/ODS/Silica (Figure 1b,c) in the Free O−H Stretching Region

A_i	Γ_i (cm^{-1})	$(T_2)_i$ (fs)	ω_i (cm^{-1})	$(\Gamma_{inh})_i$ (cm^{-1})
0.1	200	26	3600	7
−1.0	22	240	3681	1
0.30	55	96	3780	5

vibrational mode centered at 3681 cm^{-1} was found to be ∼240 fs from the simultaneous fit of SFG spectrum and SFG-FID. The relatively fast dephasing of the mode at ∼3681 cm^{-1} for the water/ODS-coated silica interface is similar to the previous report of dephasing of this mode (∼300 fs)[19] estimated from the width of the free OH peak and not from an independent time-resolved experiment. In contrast, the dephasing of the interfacial free OH in this study is determined by a time-resolved vibrational spectroscopy. The observation of a contribution at ∼3780 cm^{-1} is an indication of unreacted Si−OH groups of the silica surface[57] during the self-assembly process. It should be noted that even with an all-trans ODS SAM, there probably remain some unreacted Si−OH groups on the silica surface or on the ODS molecules.[43]

While most of the sample area (∼80%, referred to as spot A) showed the SFG spectrum and the associated short SFG-FID displayed in Figure 1, we observed a different SFG spectrum (Figure 2b) and SFG-FID (Figure 2c) in the free OH region in

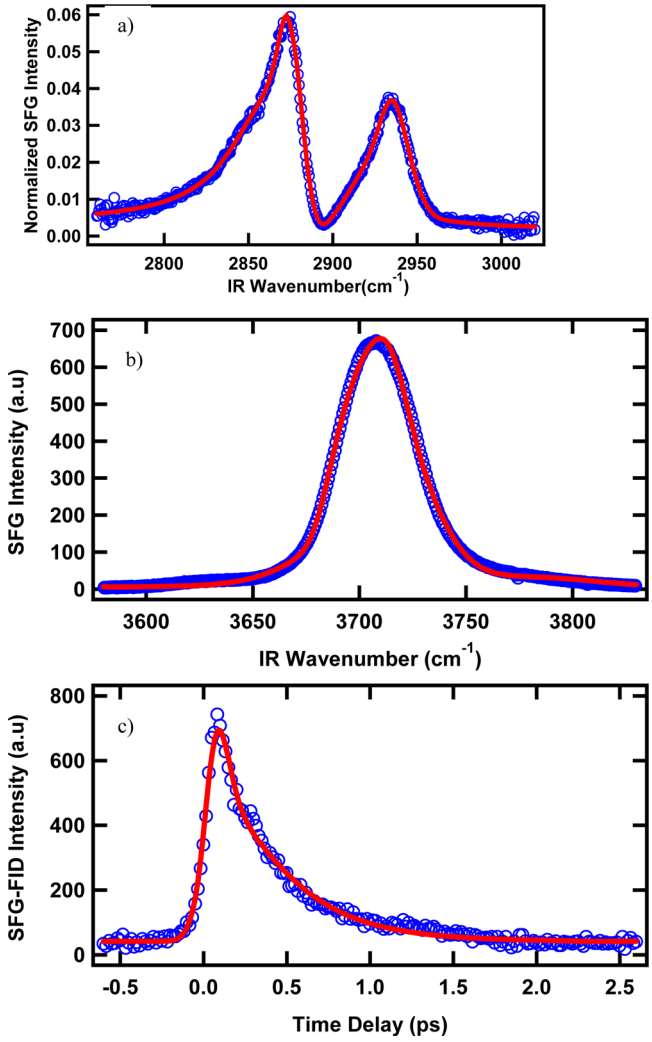

Figure 2. (a) SFG spectrum of OTS-coated silica interface in contact with H_2O in the C−H stretching region at different sample position that is shown in Figure 1. (b) SFG spectrum and (c) SFG-FID of OTS-coated silica interface in contact with H_2O in the free O−H stretching region (∼3700 cm^{-1}) at a different sample position than that shown in Figure 1. The polarization combination for SFG, vis, and IR is S,S,P.

some sample areas (∼20%, referred to as spot B) when the sample position was moved laterally along the axis of the prism, perpendicular to the visible and IR beams. In particular, at spot B, the SFG spectrum (Figure 2b) intensity is larger by more than a factor of 3 and, more interestingly, the peak position is slightly blue-shifted and the coherence time observed in the SFG-FID is much longer than observed at spot A (Figure 1). The different coherence time in the FID and slightly different shape in the spectrum clearly indicate the presence of different free OH species at different spots and hence spatial inhomogeneity. Despite the smaller probability of finding

dx.doi.org/10.1021/jp210090h | J. Phys. Chem. C 2012, 116, 21734−21741

spot B (~20%), this observation was reproduced with at least three different ODS samples when more than 30 measurements were performed over the period of 1 year.

It is noted that changing the sample position along the axis of the prism does not change the overlap of the IR and visible beams in time or space. This is verified by repeating the same measurements on the gold-coated silica prism where no change in the SFG intensity (or the crosscorrelation trace) was observed after translating the sample position laterally. The separation between two different spots (~0.7 mm) was more than the beam size.

To simultaneously fit both the SFG spectrum and the FID in the free OH region (Figure 2b,c), at least four frequencies, 3570, 3689, 3709, and 3770 cm^{-1}, were required (Table 4). It is noted that the spectrum and FID could not be fit simultaneously without including the components at 3689 or 3709 cm^{-1} (see Supporting Information). In addition, it was found that the two peaks at 3689 and 3709 cm^{-1} have opposite sign. Attempt to fit the spectrum and FID by restricting the amplitudes to have the same sign results in a poorer fit compared to a fit without this restriction (see Supporting Information). The dephasing times of the peaks at 3689 and 3709 cm^{-1} are 760 and 480 fs, respectively, which are significantly longer than the dephasing observed in Figure 1c. The dephasing of the peaks at ~3570 and 3770 cm^{-1} are short (~100 fs). It is clear that the long coherence of the SFG-FID is related to the peaks at 3689 and 3709 cm^{-1}.

In the C−H stretching region (Figure 2a), the amplitudes of the methyl peaks (~2875 and 2936 cm^{-1}) as well as methylene peaks (~2855 and 2915 cm^{-1}) are the same (within the error bars) for the spectra taken in sample positions where the SFG-FID in the free OH region shows short and long coherence (Table 3). This indicates that the conformation and hence the density of the alkyl chain appear to be the same in the spots A and B, and is perhaps not the source of the difference in free OH dephasing times. SFG measurements in the CH region at multiple positions and different ODS samples did not find distinct SAM structure (data are not shown). Therefore, the observed long/short dephasing of the free OH cannot be attributed to the structure of the alkyl chains of the SAM.

One explanation for the long dephasing of the free OH vibrational mode is the contribution of free OH of H_2O molecules that do not interact with the methyl group of ODS but rather interact with the air trapped between the water and ODS SAMs (Scheme 1). Numerous experiments and theories have proposed the presence of such a gap and/or nanobubbles between a hydrophobic layer and the water molecules.[10,12−15,58] The free OH peak position in the SFG spectrum of H_2O in contact with ODS-coated silica surface is ~20 cm^{-1} red-shifted from that of the air/H_2O interface, due to the interaction of water with methyl groups.[20] Therefore, the observation of the peak at 3700 cm^{-1} in the SFG spectrum at spot B, where the SFG-FID shows long coherence (Figure 2c), may be taken as an indication that this free OH does not interact with the methyl group of ODS but instead interacts with air.

The blue shift of the free OH peak in the SFG spectrum (Figure 2c) may also be explained by including the contribution of Si−OH groups of ODS molecules, i.e., alkyl-SiOH groups that are not cross-linked during the SAM formation and/or unreacted silanol groups at the silica surface (silica-SiOH) that are not bound to ODS molecules. The small amplitude of the symmetric and asymmetric methylene peaks in the SFG spectrum (Figures 1a and 2a) suggests that the ODS alkyl chain is in a nearly all-trans conformation with a high packing

Table 3. Assignment, Amplitude, Line Width, and Frequency of Modes from the Fit of the SFG Spectrum of H_2O/ODS/Silica (Figure 2a) in the C−H Stretching Region

assignments	A_i	Γ_i (cm^{-1})	ω_i (cm^{-1})
CH_2-sym (d^+)	0.4	18	2857
CH_3-sym (r^+)	0.9	3	2875
t-CH_2 (t-$d^-(0)$)	−0.5	7	2890
CH_2-asym ($d^-(\pi)$)	0.02	3	2914
CH_3−FR (r^+_{FR})	1	7	2936
CH_3-asym (r^-)	−0.14	8	2956

Table 4. Amplitude, Line Width, Dephasing, Frequency, and Inhomogeneous Broadening Line Width of the Modes from the Simultaneous Fit of the SFG Spectrum and the SFG-FID of H_2O/ODS/Silica (Figure 2b,c) in the Free O−H Stretching Region

A_i	Γ_i (cm^{-1})	T_2 (fs)	ω_i (cm^{-1})	Γ_{inh} (cm^{-1})
0.25	130	40	3570	9
1.0	7	760	3689	1
−0.50	11	480	3709	30
1.0	41	130	3770	15

Scheme 1. Schematic of Water Interacting with a Siloxane SAM Coated Silica Interface[a]

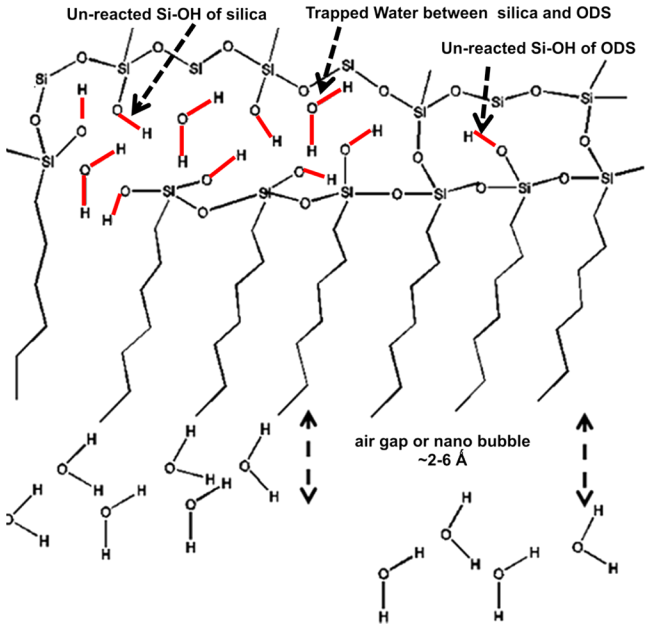

[a]The assumption is that during the self-assembly of OTS, there remain unreacted Si−OH groups either from the silica surface or from the OTS molecules. In this scheme, some water can be trapped between the ODS molecules since the monolayer can have some defects. In addition, there is a gap (2−6 Å) between the water and ODS molecules. The observed free OH in the SFG spectrum could come from the O−H of H_2O facing the hydrocarbon chain of ODS, the O−H of H_2O facing the air gap (not hydrogen bonded to other water nor interacting with the hydrocarbon chain of ODS), and the O−H of Si−OH groups of either silica or OTS and the free OH of water trapped in between the ODS molecules.

dx.doi.org/10.1021/jp210090h | J. Phys. Chem. C 2012, 116, 21734−21741

density.[54,59,60] At full coverage, the ODS molecules are not completely cross-linked because of the geometry restriction imposed by the distance between O atoms of O−Si−O (a maximum of 3.2 Å)[61,62] and the van der Waals radius of the aliphatic chain groups (3.5 Å). As a result, some Si−OH groups of the ODS molecules must be intact.[61,62] It is known from SFG spectra of ODS SAMs on glass that the frequency of Si−OH of ODS molecules lies at ∼3708 cm^{-1}.[43] We hypothesize that the blue shift of the SFG spectrum (in Figure 2b compared to Figure 1b) and the long coherence of SFG-FID of water in contact with ODS-coated silica surface (Figure 2c) can also be interpreted as the contribution of Si−OH of ODS molecules.

A third possible explanation for the observation of a long coherence in the free OH region can be due to the contribution of water molecules that are trapped within the ODS monolayer, between the ODS and silica and/or inside silica pores (Scheme 1). If there are such contributions, the confinement geometry (short distance between two ODS molecules or small pores) imposed on these water molecules will decouple them from other water molecules. As a result, the presence of distinct water molecules (those that are in direct contact with the ODS, and those that are trapped between the ODS layers and/or the ODS-silica gap) can lead to the observation of long coherences, in the SFG-FID and multiple free OH features in the SFG.

To test these hypotheses, the SFG spectrum of D_2O/ODS/silica was measured in the free OH region on spot B immediately after that of H_2O/ODS/silica. This was achieved by replacing H_2O with D_2O in the sample well under the IR fused silica prism. If the exchange between OH/OD is as fast as is in the bulk, there would not be any signal from D_2O/ODS/silica in the free OH region. However, if the exchange rate is slow, it would suggest OH species disconnected from the bulk D_2O. Interestingly, while the SFG intensity vanished almost instantaneously in spot A, we observed the persistence of SFG signal of the free OH species in spot B even after 100 min when H_2O was replaced by D_2O (Figure 3). It appears that, because

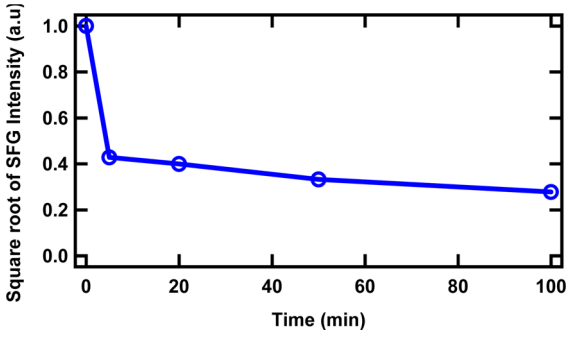

Figure 3. SFG intensity of D_2O/ODS/silica interface in the free OH region as a function of time. Time zero is when H_2O was replaced by D_2O. The SFG spectrum of the H_2O/ODS/silica interface which was measured before addition of D_2O is also shown at time zero.

of the confinement geometry of the isolated OH groups, the exchange rate with OD becomes slow, allowing nonzero SFG response to remain in the free OH region. The SFG intensity at time zero represents the silica/ODS in contact with H_2O. Right after taking the SFG spectrum of silica/ODS in contact with H_2O, the ODS/silica prism and the sample holder were removed from the setup and flushed with D_2O at least three times to exclude H_2O from the cell. The sample holder containing D_2O was then placed in contact with the ODS-coated silica prism, and the SFG spectra of D_2O/ODS/silica were recorded within 5 min and continued for up to 100 min without changing the sample position. It should be noted that this procedure did not destroy the overlap as the same experiment with H_2O resulted in the same SFG signal before and after flushing with H_2O as confirmed by the spectra in the CH stretching region which show negligible signal change.

It is clear that after a sharp decrease of the SFG signal right after exchanging with D_2O, the SFG intensity slowly decreases to an asymptotic value that is interpreted to correspond to the remaining OH groups (either from silanol or trapped water) that are isolated from the bulk D_2O and therefore cannot exchange with D_2O. The corresponding SFG-FID of the D_2O/ODS/silica in the free OH region shows a long coherence, similar to that observed in Figure 2 (see Supporting Information). The observation of the long dephasing confirms that the signal is due to the OH resonance and not just the nonresonant background. These observations suggest that the OH species that shows the long dephasing in the SFG-FID is related to the species which are isolated from the bulk, most likely Si−OH of incompletely cross-linked ODS and/or water confined in the silica pores or between the monolayers. The possibility of the long dephasing due to the topmost water molecules separated by an air gap from the SAMs is excluded because the exchange of OH/OD occurs in microsecond time scale[63,64] in bulk water (nonconfined system). Hence, the H_2O molecules at the gap between the bulk water and the CH_3 groups ODS should be easily replaced by D_2O.

Evidence for the existence of water molecules under the SAM on silica surfaces has been reported by other groups.[18,42] It was concluded that water molecules can penetrate through defects in the SAM and experience the electric field of the silica surface.[18,42] Water molecules under the SAM presumably form hydrogen bonds to silanol groups of silica or to other water molecules. However, no isolated OH species under the SAM (signature of free OH) was either observed or hypothesized in those studies.

Another control experiment was performed with ODMS instead of ODS to make a SAM at the silica surface. The use of ODMS, which has only one linker group (the methoxy group), eliminates the possibility of cross-linking between molecules and formation of rafts of cross-linked ODS molecules anchored at a few points in the ODS SAM.[65] Compared to ODS SAMs, the amplitude of C−H stretching modes in the SFG spectrum of the ODMS-coated silica in contact with H_2O is approximately an order of magnitude smaller (Figure 4a). In addition, the presence of methylene peaks (∼2850 and 2920 cm^{-1}) with large amplitudes (Table 5) is an indication of a significant number of gauche defects in the ODMS SAM, suggesting a lower density of alkyl chains compared to the ODS SAM. The smaller coverage of the monolayer of ODMS compared to the ODS was also consistent with the observation of the lower contact angle for ODMS (80° or smaller) compared to the ODS (105° or larger) SAMs.

The SFG spectrum and SFG-FID of ODMS in contact with H_2O (pH ∼ 6) in the free OH region (Figure 4b,c and Table 6) are essentially similar to those of ODS observed at spot A. The SFG-FID of ODMS in the free OH region shows a short coherence and changing the sample position does not alter the SFG-FID or SFG spectrum. In no case was a long free OH SFG-FID observed from ODMS SAMs. Although the hydrophobicity of the ODMS SAM is less than the ODS SAM, which might affect the ability to sustain an air gap between the ODMS

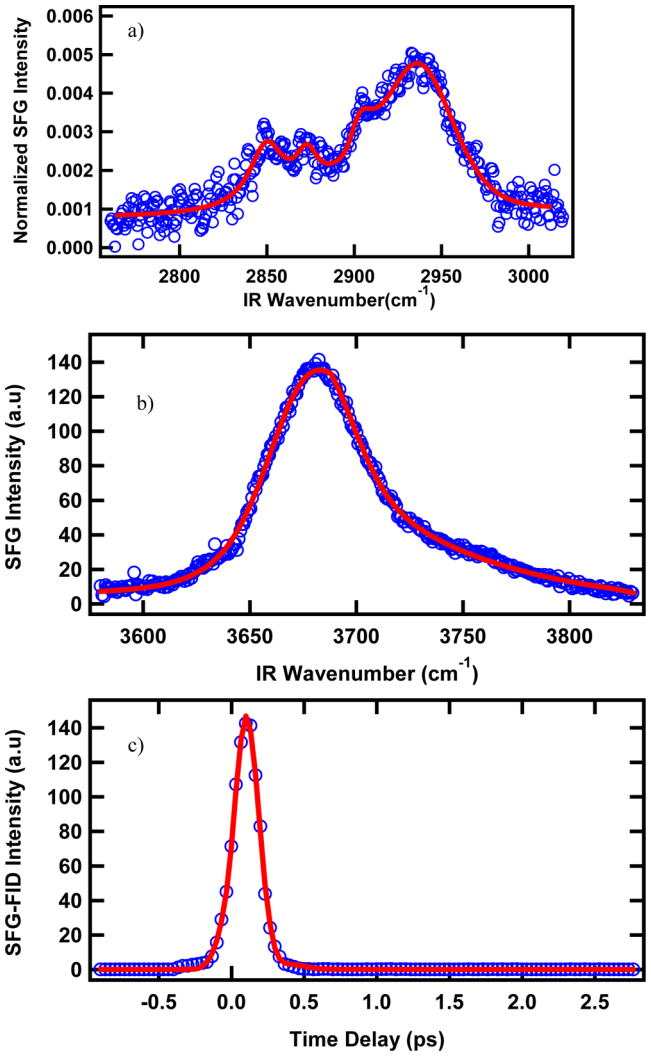

Figure 4. (a) SFG spectrum of ODMS-coated silica interface in contact with H_2O in the C−H stretching region. (b) SFG spectrum and (c) SFG-FID of ODMS-coated silica interface in contact with H_2O in the free O−H stretching region (~3700 cm^{-1}). The polarization combination for SFG, vis, and IR is S,S,P.

Table 5. Assignment, Amplitude, Line Width, and the Frequency of Modes from the Fit of the SFG Spectrum of H_2O/ODMS/Silica (Figure 4a) in the C−H Stretching Region

assignments	A_i	Γ_i (cm^{-1})	ω_i (cm^{-1})
CH_2-sym	0.26	4	2850
CH_3-sym	0.20	4	2873
t-CH_2	−0.33	7	2890
CH_2-asym	0.33	8	2914
CH_3−FR	1.0	15	2936
CH_3-asym	−0.33	20	2956

and water,[66] the absence of the long coherence in the case of ODMS SAMs in contact with water is consistent with our hypothesis that the long coherence at the ODS/water are due to the contribution of unreacted Si−OH of ODS or the water trapped in between SAM and silica surface or pores.

It is clear that much more information can be obtained from combining the time and frequency domain SFG measurements. Because the resolution of the spectra in broad-band SFG is limited by the bandwidth of the visible pulse, this approach alone is not capable of resolving bands that are separated by few wavenumbers. Time domain measurements therefore complement frequency domain experiments especially for systems that display large inhomogeneity and nonresonant contribution.

Table 6. Amplitude, Line Width, Dephasing, Frequency, and Inhomogeneous Broadening Line Width of the Modes from the Simultaneous Fit of the SFG Spectrum and the SFG-FID of H_2O/ODMS/Silica (Figure 4b,c) in the Free O−H Stretching Region

A_i	Γ_i (cm^{-1})	$(T_2)_i$ (fs)	ω_i (cm^{-1})	$(\Gamma_{inh})_i$ (cm^{-1})
1.0	68	78	3550	19
1.0	24	220	3678	7
−0.25	43	123	3777	2

CONCLUSION

The combination of frequency and time domain SFG was used to study the non-hydrogen-bonded spectral region of water at hydrophobic surfaces of ODS-coated silica. In contrast to previous studies of this system, where only one free OH peak (~3680 cm^{-1}) with short dephasing was observed, an additional peak whose frequency is blue-shifted by ~20 cm^{-1} was observed. The dephasing of this new peak is significantly slower (~760 fs) than the free OH of water in contact with ODS. Although it is challenging to make a unique assignment for the nature of the oscillator responsible for the observation of the peak at ~3700 cm^{-1} characterized by the long dephasing, isotopic exchange experiments as well as the behavior of H_2O in contact with ODMS-coated silica suggest that the OH species responsible are possibly Si−OH groups of ODS, water trapped in silica pores, water in between ODS molecules, and/or water confined between the ODS and the silica surface.

ASSOCIATED CONTENT

Supporting Information

Details of the importance of inhomogeneous broadening in simultaneous fitting, justification of the number of distinct oscillators in the simultaneous fit of FID and spectrum, the Fourier transform (FT) of the SFG spectra, and the SFG-FID of D_2O/ODS-coated silica in the free OH region (3700 cm^{-1}). This material is available free of charge via the Internet at http://pubs.acs.org.

AUTHOR INFORMATION

Corresponding Author

*Tel.: 1-215-204-9696. Fax: 1-215-204-9530. E-mail: eborguet@temple.edu.

Present Addresses

†Department of Chemistry, University of California, Berkeley, CA 94720.

‡Molecular Spectroscopy Laboratory, RIKEN, 2-1 Hirosawa, Wako 351-0198, Japan.

Notes

The authors declare no competing financial interest.

ACKNOWLEDGMENTS

This work was supported by the NSF and ACS-PRF.

REFERENCES

(1) Berne, B. J.; Weeks, J. D.; Zhou, R. H. *Annu. Rev. Phys. Chem.* **2009**, *60*, 85.
(2) Ball, P. *Chem. Rev.* **2008**, *108*, 74.
(3) Israelachvili, J.; Wennerstrom, H. *Nature* **1996**, *379*, 219.
(4) Pal, S. K.; Peon, J.; Zewail, A. H. *Proc. Natl. Acad. Sci. U.S.A.* **2002**, *99*, 1763.
(5) Lum, K.; Chandler, D.; Weeks, J. D. *J. Phys. Chem. B* **1999**, *103*, 4570.
(6) Chandler, D. *Nature* **2005**, *437*, 640.
(7) Granick, S.; Bae, S. C. *Science* **2008**, *322*, 1477.
(8) Huang, D. M.; Chandler, D. *J. Phys. Chem. B* **2002**, *106*, 2047.
(9) Godawat, R.; Jamadagni, S. N.; Garde, S. *Proc. Natl. Acad. Sci. U.S.A.* **2009**, *106*, 15119.
(10) Doshi, D. A.; Watkins, E. B.; Israelachvili, J. N.; Majewski, J. *Proc. Natl. Acad. Sci. U.S.A.* **2005**, *102*, 9458.
(11) Maccarini, M.; Steitz, R.; Himmelhaus, M.; Fick, J.; Tatur, S.; Wolff, M.; Grunze, M.; Janecek, J.; Netz, R. R. *Langmuir* **2007**, *23*, 598.
(12) Mezger, M.; Reichert, H.; Schoder, S.; Okasinski, J.; Schroder, H.; Dosch, H.; Palms, D.; Ralston, J.; Honkimaki, V. *Proc. Natl. Acad. Sci. U.S.A.* **2006**, *103*, 18401.
(13) Poynor, A.; Hong, L.; Robinson, I. K.; Granick, S.; Zhang, Z.; Fenter, P. A. *Phys. Rev. Lett.* **2006**, *97*, 266101.
(14) Mezger, M.; Sedlmeier, F.; Horinek, D.; Reichert, H.; Pontoni, D.; Dosch, H. *J. Am. Chem. Soc.* **2010**, *132*, 6735.
(15) Giovambattista, N.; Debenedetti, P. G.; Rossky, P. J. *J. Phys. Chem. B* **2007**, *111*, 9581.
(16) Netzer, L.; Iscovici, R.; Sagiv, J. *Thin Solid Films* **1983**, *99*, 235.
(17) Netzer, L.; Sagiv, J. *J. Am. Chem. Soc.* **1983**, *105*, 674.
(18) Ye, S.; Nihonyanagi, S.; Uosaki, K. *Phys. Chem. Chem. Phys.* **2001**, *3*, 3463.
(19) McGuire, J. A.; Shen, Y. R. *Science* **2006**, *313*, 1945.
(20) Tian, C. S.; Shen, Y. R. *Proc. Natl. Acad. Sci. U.S.A.* **2009**, *106*, 15148.
(21) Shen, Y. R.; Ostroverkhov, V. *Chem. Rev.* **2006**, *106*, 1140.
(22) Richmond, G. L. *Chem. Rev.* **2002**, *102*, 2693.
(23) Gopalakrishnan, S.; Liu, D. F.; Allen, H. C.; Kuo, M.; Shultz, M. J. *Chem. Rev.* **2006**, *106*, 1155.
(24) Eisenthal, K. B. *Chem. Rev.* **1996**, *96*, 1343.
(25) Du, Q.; Freysz, E.; Shen, Y. R. *Science* **1994**, *264*, 826.
(26) Peremans, A.; Tadjeddine, A. *Phys. Rev. Lett.* **1994**, *73*, 3010.
(27) Bain, C. D. *J. Chem. Soc., Faraday Trans.* **1995**, *91*, 1281.
(28) Gragson, D. E.; McCarty, B. M.; Richmond, G. L. *J. Phys. Chem.* **1996**, *100*, 14272.
(29) Baldelli, S.; Schnitzer, C.; Campbell, D. J.; Shultz, M. J. *J. Phys. Chem. B* **1999**, *103*, 2789.
(30) Yeganeh, M. S.; Dougal, S. M.; Pink, H. S. *Phys. Rev. Lett.* **1999**, *83*, 1179.
(31) Kim, J.; Cremer, P. S. *J. Am. Chem. Soc.* **2000**, *122*, 12371.
(32) Liu, D. F.; Ma, G.; Levering, L. M.; Allen, H. C. *J. Phys. Chem. B* **2004**, *108*, 2252.
(33) Tyrode, E.; Johnson, C. M.; Kumpulainen, A.; Rutland, M. W.; Claesson, P. M. *J. Am. Chem. Soc.* **2005**, *127*, 16848.
(34) Sovago, M.; Vartiainen, E.; Bonn, M. *J. Chem. Phys.* **2009**, *131*, 161107.
(35) Du, Q.; Superfine, R.; Freysz, E.; Shen, Y. R. *Phys. Rev. Lett.* **1993**, *70*, 2313.
(36) Gragson, D. E.; McCarty, B. M.; Richmond, G. L. *J. Am. Chem. Soc.* **1997**, *119*, 6144.
(37) Gan, W.; Wu, D.; Zhang, Z.; Guo, Y.; Wang, H. F. *Chin. J. Chem. Phys.* **2006**, *19*, 20.
(38) Stiopkin, I. V.; Weeraman, C.; Pieniazek, P. A.; Shalhout, F. Y.; Skinner, J. L.; Benderskii, A. V. *Nature* **2011**, *474*, 192.
(39) Wei, X.; Miranda, P. B.; Zhang, C.; Shen, Y. R. *Phys. Rev. B* **2002**, *66*, 085401.
(40) Scatena, L. F.; Brown, M. G.; Richmond, G. L. *Science* **2001**, *292*, 908.
(41) Scatena, L. F.; Richmond, G. L. *J. Phys. Chem. B* **2004**, *108*, 12518.
(42) Hopkins, A. J.; McFearin, C. L.; Richmond, G. L. *J. Phys. Chem. C* **2011**, *115*, 11192.
(43) Wolfrum, K.; Lobau, J.; Laubereau, A. *Appl. Phys. A—Mater. Sci. Process.* **1994**, *59*, 605.
(44) Roke, S.; Kleyn, A. W.; Bonn, M. *Chem. Phys. Lett.* **2003**, *370*, 227.
(45) Bordenyuk, A. N.; Jayathilake, H.; Benderskii, A. V. *J. Phys. Chem. B* **2005**, *109*, 15941.
(46) Curtis, A. D.; Burt, S. R.; Calchera, A. R.; Patterson, J. E. *J. Phys. Chem. C* **2011**, *115*, 11550.
(47) Curtis, A. D.; Asplund, M. C.; Patterson, J. E. *J. Phys. Chem. C* **2011**, *115*, 19303.
(48) Lagutchev, A. S.; Song, K. J.; Huang, J. Y.; Yang, P. K.; Chuang, T. J. *Chem. Phys.* **1998**, *226*, 337.
(49) Ye, T.; Wynn, D.; Dudek, R.; Borguet, E. *Langmuir* **2001**, *17*, 4497.
(50) Nihonyanagi, S.; Eftekhari-Bafrooei, A.; Hines, J.; Borguet, E. *Langmuir* **2008**, *24*, 5161.
(51) Eftekhari-Bafrooei, A.; Borguet, E. *J. Am. Chem. Soc.* **2010**, *132*, 3756.
(52) Gragson, D. E.; Richmond, G. L. *J. Phys. Chem. B* **1998**, *102*, 3847.
(53) Wei, X.; Wei, X.; Hong, S. C.; Lvovsky, A. I.; Held, H.; Shen, Y. R. *J. Phys. Chem. B* **2000**, *104*, 3349.
(54) Goates, S. R.; Schofield, D. A.; Bain, C. D. *Langmuir* **1999**, *15*, 1400.
(55) Macphail, R. A.; Strauss, H. L.; Snyder, R. G.; Elliger, C. A. *J. Phys. Chem.* **1984**, *88*, 334.
(56) Nihonyanagi, S.; Eftekhari-Bafrooei, A.; Borguet, E. *J. Chem. Phys.* **2011**, *134*, 084701.
(57) Morrow, B. A.; McFarlan, A. J. *J. Phys. Chem.* **1992**, *96*, 1395.
(58) Poynor, A.; Hong, L.; Robinson, I. K.; Granick, S.; Zhang, Z.; Fenter, P. A. *Phys. Rev. Lett.* **2006**, 97.
(59) Chow, B. C.; Ehler, T. T.; Furtak, T. E. *Appl. Phys. B* **2002**, *74*, 395.
(60) Ji, N.; Ostroverkhov, V.; Chen, C. Y.; Shen, Y. R. *J. Am. Chem. Soc.* **2007**, *129*, 10056.
(61) Stevens, M. J. *Langmuir* **1999**, *15*, 2773.
(62) Maoz, R.; Cohen, H.; Sagiv, J. *Langmuir* **1998**, *14*, 5988.
(63) Park, S. C.; Jung, K. H.; Kang, H. *J. Chem. Phys.* **2004**, *121*, 2765.
(64) Roose, P.; Van Craen, J.; Eisendrath, H. *Colloids Surf. A: Physicochem. Eng. Aspects* **1998**, *145*, 213.
(65) Lee, S. H.; Saito, N.; Takai, O. *Jpn. J. Appl. Phys. Part 1—Reg. Pap. Brief Commun. Rev. Pap.* **2007**, *46*, 1118.
(66) Chattopadhyay, S.; Uysal, A.; Stripe, B.; Ha, Y. G.; Marks, T. J.; Karapetrova, E. A.; Dutta, P. *Phys. Rev. Lett.* **2010**, *105*, 037803.

NOTE ADDED AFTER ASAP PUBLICATION

This paper was published to the Web on October 8, 2012, with an error to the TOC and Abstract graphic. The corrected version was reposted with the issue on October 18, 2012.